Osteoarthritis and Cartilage 23 (2015) 280–288

Osteoarthritis and Cartilage

Utility of T2 mapping and dGEMRIC for evaluation of cartilage repair after allograft chondrocyte implantation in a rabbit model

J. Endo † *, A. Watanabe † a, T. Sasho † a, S. Yamaguchi † a, M. Saito † a, R. Akagi † a, Y. Muramatsu † a, S. Mukoyama † a, J. Katsuragi † a, Y. Akatsu † a, T. Fukawa † a, T. Okubo ‡ b, F. Osone ‡ b, K. Takahashi † a

† Department of Orthopaedic Surgery, Graduate School of Medicine, Chiba University, 1-8-1 Inohana, Chuo-ku, Chiba 260-8670, Japan
‡ Department of Medical Imaging, Teikyo University Chiba Medical Center, 3426-3 Anegasaki, Ichihara, Chiba 299-0111, Japan

ARTICLE INFO

Article history:
Received 25 June 2014
Accepted 23 October 2014

Keywords:
Magnetic resonance imaging
T2 mapping
dGEMRIC
Osteochondral defect
Allograft chondrocyte implantation
Cartilage repair

SUMMARY

Objective: To investigate the effectiveness of quantitative Magnetic resonance imaging (MRI) for evaluating the quality of cartilage repair over time following allograft chondrocyte implantation using a three-dimensional scaffold for osteochondral lesions.
Design: Thirty knees from 15 rabbits were analyzed. An osteochondral defect (diameter, 4 mm; depth, 1 mm) was created on the patellar groove of the femur in both legs. The defects were filled with a chondrocyte-seeded scaffold in the right knee and an empty scaffold in the left knee. Five rabbits each were euthanized at 4, 8, and 12 weeks and their knees were examined *via* macroscopic inspection, histological and biochemical analysis, and quantitative MRI (T2 mapping and dGEMRIC) to assess the state of tissue repair following allograft chondrocyte implantation with a three-dimensional scaffold for osteochondral lesions.
Results: Comparatively good regenerative cartilage was observed both macroscopically and histologically. In both chondrocyte-seeded and control knees, the T2 values of repair tissues were highest at 4 weeks and showed a tendency to decrease with time. ΔR1 values of dGEMRIC also tended to decrease with time in both groups, and the mean ΔR1 was significantly lower in the CS-scaffold group than in the control group at all time points. $\Delta R1 = 1/r\ (R1post - R1pre)$, where r is the relaxivity of Gd-DTPA^{2-}, $R1 = 1/T1$ (longitudinal relaxation time).
Conclusion: T2 mapping and dGEMRIC were both effective for evaluating tissue repair after allograft chondrocyte implantation. ΔR1 values of dGEMRIC represented good correlation with histologically and biochemically even at early stages after the implantation.

Introduction

Articular cartilage is optimized to reduce friction and distribute weight evenly throughout the joint. It is hypocellular, with only 4% of its wet weight consisting of chondrocytes. Its main components are water and the extracellular matrix (ECM); the latter is composed of type II collagen (15–20% of weight) and proteoglycans (3–10% of weight). The protein cores of proteoglycans are lined by covalent attachments to glycosaminoglycans (GAG)[1]. However, the ability of articular cartilage to repair itself after injury is very limited[2]. Numerous strategies have been used to induce cartilage repair at damaged sites, including microfracture[3], subchondral drilling[4], osteochondral autograft transplantation[5], allograft chondrocyte implantation[6], and autologous chondrocyte implantation (ACI)[7]. ACI is generally understood as the most effective of these methods for repairing hyaline articular cartilage[7]. Good clinical results have been reported in long-term follow-up studies[8]. Yet cartilage defects repaired by ACI are not always repaired with hyaline or hyaline-like cartilage: some are repaired by fibrous cartilage, which could reduce long-term durability[7]. In addition, ACI has certain disadvantages: it requires two surgical interventions as well

* Address correspondence and reprint requests: J. Endo, Department of Orthopaedic Surgery, Graduate School of Medicine, Chiba University, 1-8-1 Inohana, Chuo-ku, Chiba 260-8670, Japan. Tel: 81-43-226-2117; Fax: 81-43-226-2116.
E-mail address: orthopaedics@hotmail.co.jp (J. Endo).
[a] Tel: 81-43-226-2117; Fax: 81-43-226-2116.
[b] Tel: 81-043-623-1711; Fax: 81-046-23-3080.

http://dx.doi.org/10.1016/j.joca.2014.10.012
1063-4584/

as *in-vitro* cell expansion, steps which lead to higher costs, longer recovery times, and the risk of cellular dedifferentiation[7]. Moreover, it can be somewhat difficult for elderly people to obtain sufficient numbers of chondrocytes with adequate differentiation potency[7]. A previous study proved the importance of chondrocyte proliferation potency not only at the recipient site but also at the donor site[9]. The cartilage was more successfully regenerated when allogenic chondrocytes from young rabbits rather than matured rabbits were used.

In addition to cell source-related issues, the cell culture scaffold is an important factor in cartilage repair. In first generation ACI, cultured chondrocytes are injected beneath a periosteal flap sutured to the edges of the prepared chondral defect. This method can cause loss of implanted cells into the joint cavity and uneven cell distribution[10,11]. In addition, the resulting monolayer culture is mechanically too weak to maintain a desired shape and structure. An allograft chondrocyte implantation technique using a three-dimensional scaffold could allay some of these concerns and satisfy the growing clinical demand[6]. It should be noted, however, that allograft chondrocyte implantation using a three-dimensional scaffold might elicit an immune response, as the cell source is an allograft and the scaffold is a foreign substance[6]. Moreover, this technique is not necessary associated with the best cartilage regeneration. Therefore, investigating how implanted chondrocytes engraft over time is an important step in determining the clinical usefulness and application of this promising procedure. Meanwhile, quantitative evaluation of tissue repair has been rather difficult because of a lack of noninvasive methods for monitoring tissue status.

Magnetic resonance imaging (MRI) is a noninvasive method of evaluating regenerated cartilage; conventional MR imaging techniques for cartilage have mainly been used for morphological evaluation[12]. In recent years, quantitative MRI techniques have been developed as monitoring the cartilage matrix status[13]. T2 mapping[14], delayed gadolinium-enhanced MR imaging of cartilage (dGEMRIC)[15], T1rho mapping[16], and diffusion-weighted imaging (DWI) have been introduced as effective methods of evaluating regenerative cartilage[17]. Previous studies have clarified the relationships between quantitative MRI techniques and biochemical assessments. T2 values indicate comprehensive cartilage status, including water concentration, proteoglycan concentration (principally, aggrecan measured as GAG), and collagen anisotropy[15]. dGEMRIC highlights the changes in GAG concentration that occur in degenerative cartilage in association with OA[18,19]. To date, however, no systematic study has evaluated cartilage repair over time through histological and biochemical analysis as well as through quantitative MRI. The aim of this study is to investigate the utility of quantitative MRI for evaluation of the quality of repaired tissues at several time points following allograft chondrocyte implantation using a three-dimensional scaffold for osteochondral lesions.

Materials and methods

Isolation and cultivation of chondrocytes

Healthy native cartilage was extracted from two New Zealand white rabbits (male, 6 weeks old, average weight 1.5 kg). The rabbits were anesthetized, and articular cartilage slices from the knee and shoulder joints were mixed for *in-vitro* culture as described in previous studies[6]. The chondrocytes were liberated by sequential digestion with pronase (Kaken Pharmaceutical Inc., Tokyo, Japan) or collagenase (Kaken Pharmaceutical Inc., Tokyo, Japan). The digested tissue was passed through a cell strainer (Becton Dickinson Labware Co. Ltd., Franklin Lakes, NJ, USA) with a pore size of 40 μm. The filtrate was centrifuged at 1500 rpm for 10 min to separate the cells. The 4×10^6 harvested chondrocyte cells were cultured with 15 three-dimensional atelocollagen honeycomb-shaped scaffolds (with 1 mm thickness and 4 mm diameter, KOKEN Inc., Tokyo, Japan) in DMEM/F12 supplemented with 20% fetal bovine serum and 50 g/mL ascorbic acid (Sigma–Aldrich, St. Louis, MO, USA) at 37°C in an atmosphere of 5% CO_2 in air for 2 weeks. Preparation of the scaffold was performed in accordance with the method described by Masuoka *et al.*[6]. They investigated the quality of allograft chondrocyte implantation using the same types of scaffolds used in this study, and showed that cartilage cultured *in vitro* for 14 days retained sufficient elasticity and stiffness to be handled *in vivo*[6]. The cell-containing cultured scaffold was called a chondrocyte-seeded scaffold (CS-scaffold).

Transplantation of chondrocytes

Fifteen New Zealand white rabbits (male, 12 weeks old, average weight 2 kg) were anesthetized with 3 ml of a mixture of 0.5% xylazine and 7.5% ketamine. Osteochondral lesions that completely penetrated the entire subchondral bone (1 mm depth, 4 mm diameter) were drilled on the patellar groove of the femur in both legs using a low-speed drill. The defects were filled with a CS scaffold in the right knee and with an empty scaffold (control) in the left knee. No periosteal patch or fibrin glue was used to attach the scaffold to the defect. Five rabbits each were euthanized at 4, 8, and 12 weeks postoperatively.

Sample preparation for MRI

The rabbits were euthanized at the indicated postoperative time points. The distal femurs including the operated sites were sawn into pieces, each containing a single defective area. Sample preparation for T2 mapping and dGEMRIC was performed as described in previously reported studies[18,20]. Each specimen was placed into a plastic tube that contained 0.9% normal saline kept at the ambient temperature of the MRI room. T2 mapping and pre-contrast MRI for dGEMRIC were performed, after which each specimen was placed into a plastic bottle containing 10 ml of 0.5 mM gadopentetate dimeglumine ($Gd\text{-}DTPA^{2-}$; Magnevist®; Schering, Berlin, Germany) in 0.9% normal saline. These plastic bottles were placed into a refrigerator at 4°C and equilibrated overnight with continuous stirring. Each specimen was then placed into a plastic tube containing 0.5 mM $Gd\text{-}DTPA^{2-}$ in 0.9% normal saline, which was kept at the ambient temperature of the MRI room. Post-contrast MR imaging was then performed.

MR imaging

MR imaging was performed with an MR imaging system at 1.5 T (GE Healthcare, Milwaukee, WI, USA) with a custom-made, receive-only, 30-mm-diameter solenoid coil. For dGEMRIC, R1 pre-contrast (R1pre) and R1post-contrast (R1post) measurements were performed according to the methods described in a previous study[15]. The local concentration of $Gd\text{-}DTPA^{2-}$ penetrating the tissue is governed by the equation: $[Gd\text{-}DTPA^{2-}] = 1/r\ (R1post - R1pre)$, where r is the relaxivity of $Gd\text{-}DTPA^{2-}$, $R1 = 1/T1$ (longitudinal relaxation time). R1 measurement was performed using a fast-spin-echo inversion-recovery sequence (2670 ms repetition time, 14 ms echo time, seven inversion times of 40, 80, 160, 320, 640, 1280, and 2560 ms, 30 × 30 mm field of view, 1.0 mm section thickness, 384 × 384 matrix, and 130 kHz bandwidth). T2 measurement was performed using a multi-spin-echo sequence (1500 ms repetition time, 10 echo times of 10.9–109 ms,

30 × 30 mm field of view, 1.0 mm slice thickness, 384 × 384 matrix, and 280 kHz bandwidth). Single-slice acquisition was used for both R1 and T2 measurements to exclude undesirable factors such as magnetization transfer and cross-talk[9,10], both of which might occur if multislice acquisition were used. Pre-contrast MR imaging of the prepared specimen was performed on the day of euthanasia. On the following day, post-contrast MR imaging of the prepared specimen was performed. The R1post measurement was performed in the same manner as the R1pre measurement. For the R1post measurement and T2 measurement, the corresponding slice that was used for the R1pre measurement was identified carefully based on the morphological images, which were acquired repeatedly if needed.

Imaging analysis

Imaging analysis for dGEMRIC and T2 mapping was performed as described in a previously reported study[15]. R1pre, R1post, and the difference between R1pre and R1post (ΔR1)-calculated maps, as well as T2-calculated maps, were generated using MATLAB (The MathWorks, Natick, MA, USA) with a mono-exponential curve fit. In MATLAB, color-coded R1- and T2-calculated maps of the cartilage, segmented manually, were overlaid on the inversion-recovery image, which had an inversion time of 2560 ms, and on the MSE image, which had an echo time of 21.8 ms. For R1 and T2 measurements, the region of interest containing repaired tissue was drawn manually over the whole repair site by a single musculoskeletal radiologist, who was blind to the type of scaffold implanted in each sample and the duration of the *in-vivo* culturing period.

Histological and biochemical evaluations

After MRI, the distal femurs were washed with saline. Each specimen was sectioned into halves through the center of the repair site. One half of the repaired tissue was used for histological evaluation according to the Kawamoto procedure[21]. The sections were evaluated microscopically and scored according to a histological grading scale in five categories with a total score ranging from 0 to 14 points as described by Wakitani and colleagues (Table I)[22]. The other half of the specimen was harvested using scalpels and curettes and used for biochemical evaluations. The GAG concentration was measured by means of high performance liquid chromatography (HPLC). HPLC procedures were performed in accordance with the method described by Frazier *et al.*[23].

Statistical analysis

The data were analyzed with the SPSS statistical package (SPSS, Chicago, IL, USA). The Wakitani score, GAG concentration, T1 value, and T2 value were compared between the control group and the CS-scaffold group by the Mann–Whitney *U* test. Values at different time points in the same group were compared using the Kruskal–Wallis test and the Steel–Dwass *post-hoc* test. The relationship between GAG concentration and the R1post and ΔR1 was compared by regression analysis. Statistical significance was defined as $P < 0.05$.

Table I
Wakitani score

A. Cell morphology	(0–4)
B. Matrix staining	(0–3)
C. Surface regularity	(0–3)
D. Thickness of cartilage	(0–2)
E. Integration of donor with host adjacent cartilage	(0–2)

Total 14 points.

Results

In-vitro cultivation of chondrocytes with scaffold

After 2 weeks of stirred culture, macroscopic and histological assessments revealed that the scaffolds were translucent and elastic in *in-vivo* experiments. Chondrocytes in the scaffolds were homogeneous and maintained their typical small and round histological appearance (Fig. 1).

Macroscopic examination

In this study, a total of 15 rabbits were euthanized at 4, 8, and 12 weeks postoperatively. Macroscopically, there was no sign of immunogenic reaction, infection, or deviation of implanted scaffold. After 4 weeks *in vivo*, all five samples exhibited partial hemorrhage. In the CS-scaffold group, on the other hand, parts of the repaired tissues appeared translucent. After 8 weeks *in vivo*, white fibrous tissues were seen in parts of the repaired lesion in the control group; in the CS-scaffold group, in contrast, the repaired tissues resembled the surrounding native hyaline cartilage. After 12 weeks *in vivo*, further maturation was seen in both groups, and there was almost no difference between the control and CS-scaffold group (Fig. 2).

Histological and biochemical evaluations

After 4 weeks *in vivo*, the scaffold structure in the control group appeared to be nearly empty, little cellular infiltration could be seen. In the CS-scaffold group, in contrast, chondrocytes and ECM, both dyed a deep blue with toluidine blue, were seen in parts of the repaired tissue. After 8 weeks *in vivo*, the defects were filled with fibrocartilage, though the surface was irregular in both groups. The cellular density and the concentration of ECM stained with toluidine blue had increased more dramatically in the CS-scaffold group than in the control group. After 12 weeks *in vivo*, the repair tissues had matured further in both groups, especially in the CS-scaffold group, where the tissues were completely filled with reparative tissue resembling hyaline cartilage (Fig. 3). A semi-quantitative histological evaluation was scored according to the Wakitani score. The repairing tissues in both the control group and the CS-scaffold group matured with time between 4 and 12 weeks, but at all time points the tissues in the CS-scaffold group were significantly more mature than those in the control group (Fig. 4, Table II). The biochemical assessments were performed by means of GAG assay. GAG concentrations in both groups increased over time from 4 to 12 weeks (Table II).

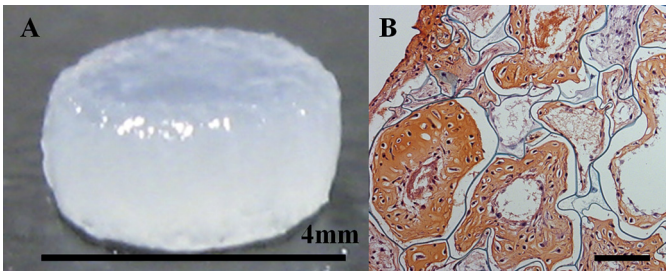

Fig. 1. Representative appearance of the chondrocyte-seeded scaffold (CS-scaffold) after 2 weeks *in-vitro* cultivation. (A) Histological observation of the CS-scaffold. The sample was stained with Safranin O. (B) (bar length, 100 μm).

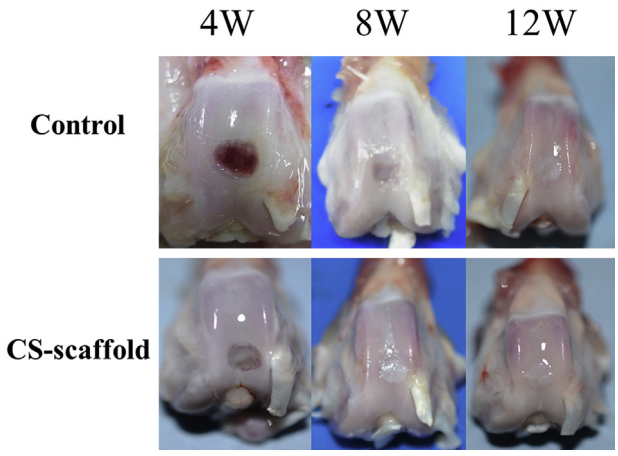

Fig. 2. Macroscopic assessment of repaired tissues of the control and CS-scaffold groups at 4, 8, and 12 weeks. The defects are filled with white fibrous tissues with time in both groups. The repaired tissues at 12 weeks resembled the surrounding native hyaline cartilage in both the control and CS-scaffold groups.

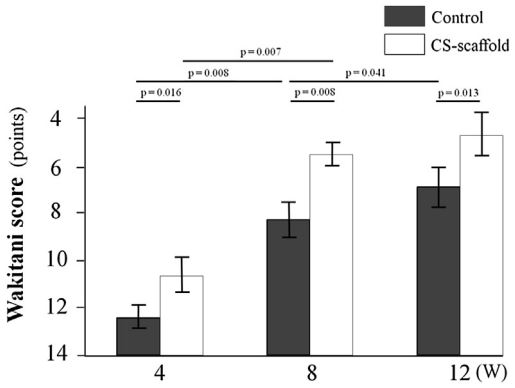

Fig. 4. Wakitani score for histological evaluation. Wakitani scores in the control and CS-scaffold groups were significantly better over time. Moreover, the CS-scaffold group was significantly better scores than control group at all time point ($P < 0.05$). Bars show the means ± 95% CI ($n = 5$ knees in each group and time point).

Quantitative MRI assessment

T2 mapping and dGEMRIC

In our repairing tissues, the T2 values in both groups were highest at 4 weeks, and showed a tendency to decrease over time [Fig. 5(A)]. A significant difference between the control and CS-scaffold groups was seen after 8 weeks [Fig. 6(A)]. As regards dGEMRIC, R1post-calculated maps of representative repair tissues are shown in Fig. 5(B). ΔR1 values showed a tendency to decrease with time in both groups, and the mean ΔR1 was significantly lower in the CS-scaffold group than in the control group at all time points ($P < 0.05$) [Fig. 6(B)].

Data analysis

The intra- and inter-observer reliability (intraclass correlation coefficients) were 0.92 (95% CI: 0.89–0.94) and 0.80 (95% CI: 0.72–0.86), respectively, for T2 mapping and 0.93 (95% CI: 0.89–0.95) and 0.81 (95% CI: 0.74–0.87) for dGEMRIC. Significantly negative correlations were observed between T2 values and Wakitani scores as well as between ΔR1 and Wakitani scores.

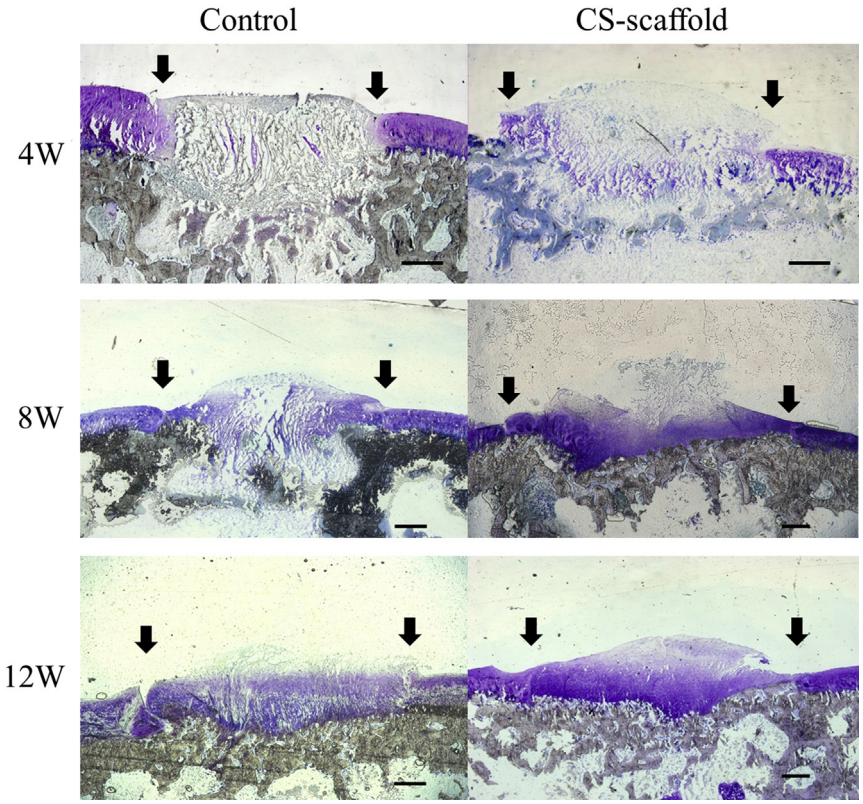

Fig. 3. Histological assessment of repaired tissues of the control and CS-scaffold groups at 4, 8, and 12 weeks. Toluidine blue staining of the implanted scaffold (bar length, 500 μm). The repair tissues matured with time in both groups. The black arrows show the border between the native lesion and repaired tissue. The integration of repair tissues with native cartilage in the CS-scaffold group was smoother in the CS-scaffold group.

Table II
Each parameter between control group and CS-scaffold group

Parameters	Control ($n = 5$ in each point)			CS-scaffold ($n = 5$ in each point)		
	4W	8W	12w	4W	8W	12W
Mean T2 values (ms)	75 (46–104)	56 (36–76)	47 (34–60)	81 (49–113)	38 (25–51)	36 (27–45)
Mean R1pre (1/S)	1.26 (1.16–1.36)	1.27 (1.09–1.45)	1.36 (1.29–1.43)	1.33 (1.26–1.40)	1.41 (1.36–1.46)	1.44 (1.40–1.48)
Mean R1post (1/S)	3.11 (2.96–3.26)	3.01 (2.85–3.17)	2.96 (2.81–3.11)	3.13 (3.00–3.26)	2.98 (2.86–3.10)	2.98 (2.85–3.11)
Mean ΔR1 (1/S)	1.85 (1.72–1.98)	1.74 (1.59–1.89)	1.59 (1.46–1.72)	1.74 (1.62–1.86)	1.57 (1.51–1.63)	1.54 (1.45–1.63)
Wakitani score (0–14 points)	12.4 (11.9–12.9)	8.2 (7.5–8.9)	6.8 (6.1–7.5)	10.6 (9.8–11.4)	5.4 (4.9–5.9)	4.6 (3.8–5.4)
GAG concentration (μg/mg)	7.7 (4.9–10.5)	15.1 (12.6–17.6)	32.7 (24.0–41.4)	11.5 (8.4–14.6)	27.9 (20.0–35.8)	48.2 (38.8–57.6)

Data are presented as the mean and 95% CI.

Significantly negative correlations were also observed between R1post and GAG concentration and between ΔR1 and GAG concentration (Fig. 7).

Discussion

In the present study, comparatively good regenerative cartilage was observed both macroscopically and histologically to results from allograft chondrocyte implantation with a three-dimensional scaffold for osteochondral lesion. The implanted tissues were seen to mature over time without triggering an immunologic response until at least 12 weeks. We selected young rabbits because their chondrocytes had good proliferation potency, and because, in a human study, cartilage was more successfully regenerated when articular chondrocytes from young subjects were used[9]. Indeed, in clinical settings, ACI has been used in rather young patients for cartilage defects after osteochondral lesions[12]. Future studies will have to test our protocol in rabbits of various ages, as the results may be changed when more mature rabbits are used. Allogenic chondrocyte implantation has several merits. It is adaptable for treatment of cartilage defects in elderly people because it provides sufficient numbers of young chondrocytes with good proliferation potency. Second, chondrocytes proliferate readily and their cell properties do not vary from one individual to another, a trait that is usually seen in mesenchymal stem cells[24]. On the other hand, allogenic recipients do have a risk of immunological rejection. One study reported that allogenic implantation of isolated rabbit chondrocytes elicits an immune response in 10 days that gradually destroys the resulting cartilage tissue[24]. Osteochondral allograft implantation; however, has demonstrated a high success rate as defined by graft survival and good/excellent patient evaluations without risk of rejection in previous studies[25,26]. This is possible partly because chondrocytes remain viable when transplanted within their dense surrounding matrix of a tissue graft or engineered construct. More specifically, the presence of an ECM is believed to form a protective barrier around the chondrocytes that blocks both the infiltration of host immune cells into the graft as well as the escape of immunogenic chondrocytes out of the graft[27]. The results of this study are not necessarily identical to the results that can be expected in human beings; it has, however, great potential to be clinically useful. Further studies will need to confirm that no immunological responses or other problems occur over a longer follow-up period after implantation.

Another important factor in cartilage repair is the choice of scaffold, and several types of scaffolds are available for use in treating cartilage injury[6,8,28]. We chose a three-dimensional atelocollagen honeycomb-shaped scaffold for our tissue engineering. The high-density three-dimensional culture system used with this scaffold allows chondrocytes to maintain their phenotypes and their ability to produce the extracellular molecules that are required for tissue reconstruction[14,29]. Chondrocytes cultivated *in vitro* in these scaffolds in the present study were homogeneous and their structure was well organized, as observed in macroscopic and histological assessments conducted 2 weeks after implantation (Fig. 1). Masuoka *et al.* investigated repaired cartilage after articular osteochondral defects using the same type of scaffold used in the current study. They found that GAG content in the scaffold was upregulated as the formation of matrix molecules in the scaffold progressed[6]. We created osteochondral lesions and implanted empty scaffolds (control) or CS-scaffolds. At 12 weeks after implantation, repaired tissues in the CS-scaffold group exhibited better histological results and GAG content compared to those in the control group. These results show that allograft chondrocyte implantation using these scaffolds should be the treatment of

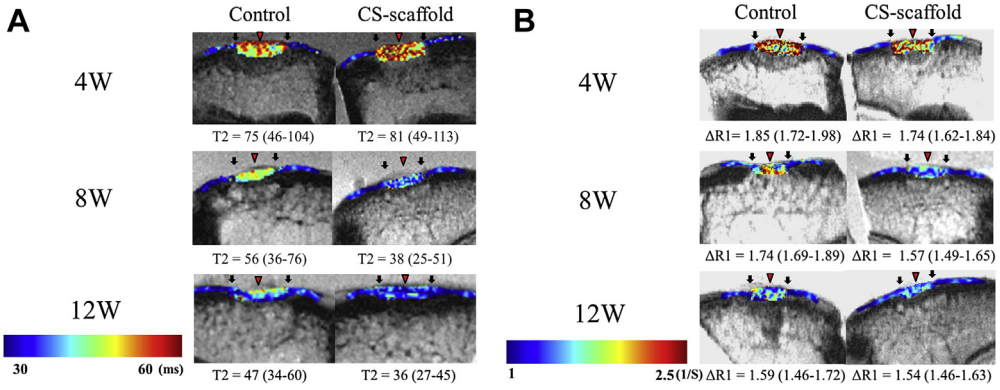

Fig. 5. A, B Color coded T2 maps and dGEMRIC (post-contrast T1 map) of representative specimens. Color coding was performed at the osteochondral defect site (arrowhead), at the border between the defect lesion and the adjacent native cartilage (arrows), and in the adjacent native cartilage. The mean T2 and T1 values of native hyaline cartilage were approximately 30 ms and 350 ms, respectively. The color mappings in control and CS-scaffold groups had tendency to represent bluer as maturing progresses in both groups. The color mappings were conducted osteochondral defect and the adjacent native cartilage. Data are presented as the mean and 95% CI ($n = 5$ knees in each group and time point).

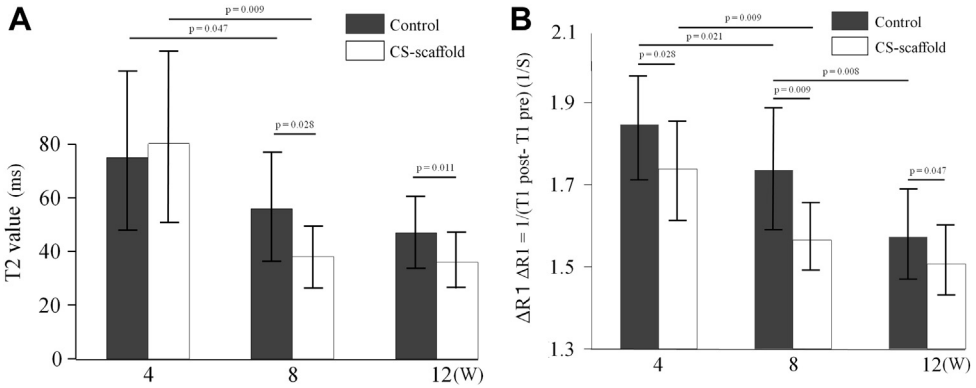

Fig. 6. A, B: The T2 values and ΔR1 showed tendency to decrease with time in both groups. The significant difference between control and CS-scaffold group were seen after 8 weeks. (A) (8W: $P = 0.028$, 12W: $P = 0.011$), the significant difference between control and CS-scaffold group were seen at all time points. (B) (4W: $P = 0.028$, 8W: $P = 0.009$, 12W: $P = 0.047$), bars show the means ± 95% CI ($n = 5$ knees in each group and time point).

choice for promoting cartilage repair. Further studies will be needed to investigate the long-term durability and human adaptability of these scaffolds.

T2 mapping

T2 mapping provides information about the interaction of water molecules and the collagen network within cartilage[13,14,30]. In animal studies, T2 mapping has been reported as a means of assessing cartilage repair. T2 values appear to be sensitive to the structural characteristics of the repaired tissue. In comparison to native cartilage, previous studies have shown that the decrease in T2 values associated with maturity of repaired tissues indicates decreased water concentration and collagen anisotropy in these tissues[14,30]. In this study, the T2 values tended to decrease over time in both the control group and the CS-scaffold group; this may represent a decrease in the water concentration and an increase in collagen anisotropy in the repaired tissue following its maturation. A significant difference between the groups was observed after 8 weeks, suggesting that the water content and the degree of collagen anisotropy were already changing in the repair tissues by this time; there is some controversy, however, regarding which

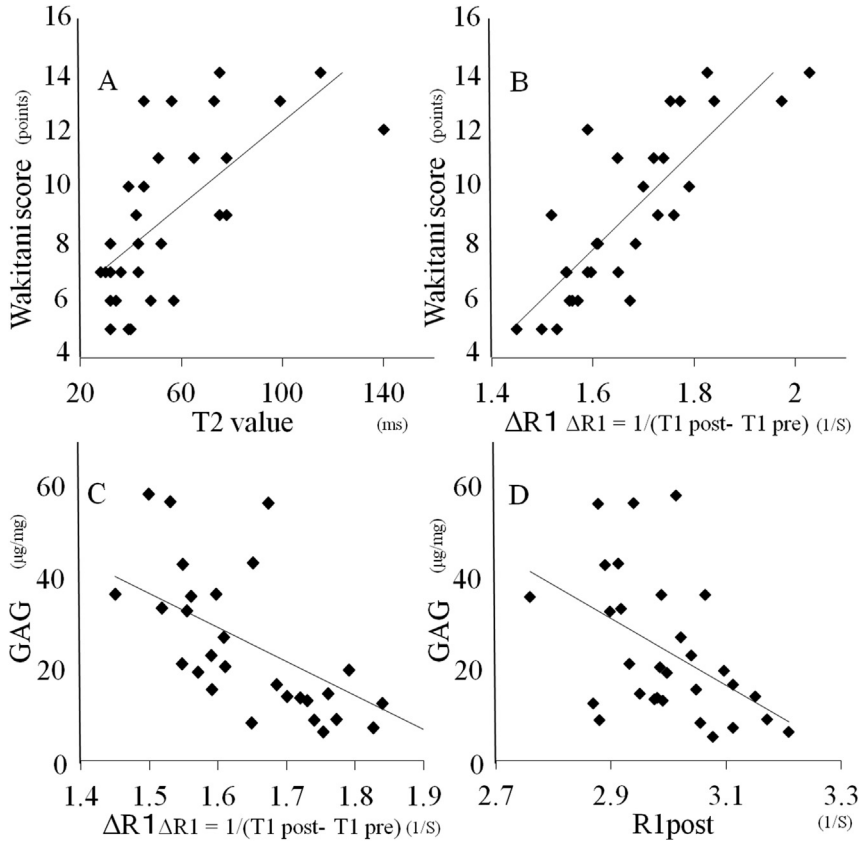

Fig. 7. Quantitative correlations between T2 values and Wakitani score in repaired tissue (A) ($r = -0.67$, $P < 0.001$), ΔR1 and Wakitani score in repaired tissue (B) ($r = -0.81$, $P < 0.001$), ΔR1 and GAG concentration (C) ($r = -0.64$, $P < 0.001$), R1 post and the GAG concentration (D) ($r = -0.47$, $P = 0.008$) ($n = 30$ in each graph).

parameter is primarily represented by the T2 values[14]. This suggests that T2 values might be an effective biomarker for the overall state of a cartilage sample, incorporating both water concentration and collagen anisotropy, rather than indicating a single parameter. A significantly negative correlation was observed between T2 values and Wakitani score ($r = -0.67$, $P < 0.001$), which also supports our considerations. In recent years, several sequences for fast T2 mapping have been introduced, such as the steady-state free precession (SSFP) technique[31]. This technique may promote the clinical application of T2 mapping.

dGEMRIC

dGEMRIC is known to be a reliable technique for evaluating GAG concentration in articular cartilage[15,32]. The protocol for T2 mapping and dGEMRIC used in this study has rapidly become an established resource in daily clinical consultation[33]. Therefore, our results could be helpful for future clinical studies. This technique seems to highlight the changes in GAG concentration that occur in degenerative cartilage in association with OA[18,19]. It has been suggested that, in repaired tissue, not only a post-contrast T1 measurement but also a pre-contrast T1 measurement was necessary to evaluate the GAG concentration, as repaired tissue has a noticeable pre-contrast T1 elevation compared to native cartilage[34,35]. In the comparison analysis of ΔR1 and R1post, a correlation was observed between ΔR1 and GAG concentration ($r = -0.64$, $P < 0.001$) as well as between R1post and GAG concentration ($r = -0.47$, $P = 0.008$). There was no significant difference between the r-values ($P = 0.363$); however, ΔR1 may be a more sensitive tool than R1post for the measurement of GAG concentrations in regenerative cartilage, as previous studies have reported[36,37]. Our results showed that the ΔR1 value tended to decrease over time in the control and CS-scaffold groups. A significant correlation ($r = -0.81$, $P < 0.001$) was observed between T2 value and Wakitani score as well as between ΔR1 value and Wakitani score ($r = -0.67$, $P < 0.001$). There was no significant difference between the r-values ($P = 0.320$). ΔR1 revealed a significant difference between the control group and the CS-scaffold group at 4 weeks, although the T2 value did not represent the significant difference until 8 weeks. The results suggest that dGEMRIC may be useful for evaluating the status of repaired cartilage at an early stage in the maturity process after chondrocyte implantation, which cannot be evaluated by T2 mapping.

Other MRI techniques

Several other MRI techniques provide reliable quantitative analysis of cartilage composition. T1rho mapping refers to the dissipation of energy by protons under the constant influence of a weak radiofrequency, or spin lock, pulse in the transverse plane[38]. This pulse locks protons in phase to sequester T2 relaxation, and protons instead relax with the time constant T1rho. The relaxation behavior of water in close proximity to large macromolecules is affected by the presence of the spin lock pulse. These water protons dissipate energy faster than free water not associated with macromolecules can. Due to these properties of T1rho relaxation, this quantitative measure is believed to be inversely correlated with PG or GAG content, providing an indication of early OA[39]. DWI has recently provided yet another quantitative technique for measuring cartilage composition. This technique measures the translational motion of extracellular water molecules by applying diffusion-sensitizing gradients that cause mobile water protons to lose phase coherence and MR signal[40]. Other MRI techniques such as sodium MRI, Ultrashort TE, and gagCEST have also been studied[41–43].

Basic research has been conducted into the usefulness of T2 mapping, dGEMRIC and T1rho mapping in evaluating regenerative cartilage; there is little systematic evidence, however, regarding the usefulness of the other MRI techniques in evaluating regenerative cartilage in basic research. A combination of these MRI techniques with either T2 mapping or dGEMRIC might be particularly useful in evaluating regenerative cartilage. Consequently, an investigation into the effectiveness of each MRI technique in evaluating regenerative cartilage is an important next step.

Our study had several limitations. First, we evaluated the specimens for only 12 postoperative weeks. We need longer follow-up times in order to evaluate the effectiveness and immunological rejection of allograft chondrocyte implantation with three-dimensional scaffold for osteochondral lesion. Second, the sample size was relatively small. It may not have been large enough to confirm the presence or absence of an immunological rejection or the large individual differences between certain tissues. Further studies are needed with larger numbers of samples. Third, the evaluation of the time-dependent change in each sample *in vitro* should be required in order to apply it clinically; yet multiple time-dependent quantitative MRI evaluations cannot be achieved in the same individual, and histological and biochemical evaluations from the same individual are also needed. Fourth, we did not evaluate the T2 and R1 pre/post values of the control and CS-scaffolds at time zero in this study, though this data might have been useful. Fifth, regions of interest between repaired tissues and reference cartilage were drawn manually. This process might have influenced the results, though we confirmed the small margin of error using intraclass correlation coefficients. Automatic segmentation may help avoid the possible measurement errors caused by manual segmentation[44]. In addition, precise measurements of relaxation time were difficult to obtain using clinical MR imaging apparatus because many factors, including inhomogeneities in the magnetic field, can affect these results. The accuracy with which relaxation time is measured is an important limitation in any study using MRI. We believe, however, that our measurements were sufficiently accurate, as we set the MRI equipment as precisely as possible.

T2 mapping and dGEMRIC were proven to be effective methods to investigate histological and biochemical parameters in this study. Moreover, these quantitative MRI methods can be used on both humans and animals; consequently, further study using time-dependent quantitative MRI in same individual would clarify the effectiveness of allograft chondrocyte implantation with three-dimensional scaffold.

Conclusion

Our results represented that both quantitative MRI methods were effective; however, ΔR1 values of dGEMRIC might be more effective than T2 mapping for evaluating repair tissues at early stage after allograft chondrocyte implantation.

Author contributions

All authors approved the final version of the manuscript.
Study conception and design: AW, TS, SY.
Acquisition of data: TO, FO.
Analysis and interpretation of the data: AW, TS.
Critical revision of the article for important intellectual content: all authors.

Conflict of interest

We have no financial conflict related to the subject matter nor materials discussed in this manuscript at any of our academic institutions or employers.

Acknowledgments

The authors would like to thank Yohey Yamamoto, Hiroko Hoshi and Toshihide Sasaki for their technical advices.

References

1. Matzat SJ, van Tiel J, Gold GE, Oei EH. Quantitative MRI techniques of cartilage composition. Quant Imaging Med Surg 2013;3:162–74.
2. Hunziker EB. Articular cartilage repair: basic science and clinical progress. A review of the current status and prospects. Osteoarthritis Cartilage 2002;10:432–63.
3. Steadman JR, Briggs KK, Rodrigo JJ, Kocher MS, Gill TJ, Rodkey WG. Outcomes of microfracture for traumatic chondral defects of the knee: average 11-year follow-up. Arthroscopy 2003;19:477–84.
4. Dzioba RB. The classification and treatment of acute articular cartilage lesions. Arthroscopy 1988;4:72–80.
5. Hangody L, Füles P. Autologous osteochondral mosaicplasty for the treatment of full-thickness defects of weight-bearing joints: ten years of experimental and clinical experience. J Bone Joint Surg Am 2003;85-A(Suppl 2):25–32.
6. Masuoka K, Asazuma T, Ishihara M, Sato M, Hattori H, Yoshihara Y, *et al*. Tissue engineering of articular cartilage using an allograft of cultured chondrocytes in a membrane-sealed atelocollagen honeycomb-shaped scaffold (ACHMS scaffold). J Biomed Mater Res B Appl Biomater 2005;75:177–84.
7. Brittberg M, Lindahl A, Nilsson A, Ohlsson C, Isaksson O, Peterson L. Treatment of deep cartilage defects in the knee with autologous chondrocyte transplantation. N Engl J Med 1994;331:889–95.
8. Peterson L, Minas T, Brittberg M, Nilsson A, Sjögren-Jansson E, Lindahl A. Two- to 9-year outcome after autologous chondrocyte transplantation of the knee. Clin Orthop Relat Res 2000:212–34.
9. Guerne PA, Blanco F, Kaelin A, Desgeorges A, Lotz M. Growth factor responsiveness of human articular chondrocytes in aging and development. Arthritis Rheum 1995;38:960–8.
10. Watanabe A, Boesch C, Obata T, Anderson SE. Effect of multislice acquisition on T1 and T2 measurements of articular cartilage at 3T. J Magn Reson Imaging 2007;26:109–17.
11. Kneeland JB, Shimakawa A, Wehrli FW. Effect of intersection spacing on MR image contrast and study time. Radiology 1986;158:819–22.
12. Moriya T, Wada Y, Watanabe A, Sasho T, Nakagawa K, Mainil-Varlet P, *et al*. Evaluation of reparative cartilage after autologous chondrocyte implantation for osteochondritis dissecans: histology, biochemistry, and MR imaging. J Orthop Sci 2007;12:265–73.
13. Loeuille D, Chary-Valckenaere I. MRI in OA: from cartilage to bone marrow lesion. Osteoporos Int 2012;23(Suppl 8):S867–9.
14. Pai A, Li X, Majumdar S. A comparative study at 3 T of sequence dependence of T2 quantitation in the knee. Magn Reson Imaging 2008;26:1215–20.
15. Watanabe A, Boesch C, Anderson SE, Brehm W, Mainil Varlet P. Ability of dGEMRIC and T2 mapping to evaluate cartilage repair after microfracture: a goat study. Osteoarthritis Cartilage 2009;17:1341–9.
16. Holtzman DJ, Theologis AA, Carballido-Gamio J, Majumdar S, Li X, Benjamin C. T(1ρ) and T(2) quantitative magnetic resonance imaging analysis of cartilage regeneration following microfracture and mosaicplasty cartilage resurfacing procedures. J Magn Reson Imaging 2010;32:914–23.
17. Friedrich KM, Mamisch TC, Plank C, Langs G, Marlovits S, Salomonowitz E, *et al*. Diffusion-weighted imaging for the follow-up of patients after matrix-associated autologous chondrocyte transplantation. Eur J Radiol 2010;73:622–8.
18. Bashir A, Gray ML, Boutin RD, Burstein D. Glycosaminoglycan in articular cartilage: in vivo assessment with delayed Gd(DTPA)(2-)-enhanced MR imaging. Radiology 1997;205:551–8.
19. Nieminen MT, Nissi MJ, Mattila L, Kiviranta I. Evaluation of chondral repair using quantitative MRI. J Magn Reson Imaging 2012;36:1287–99.
20. Bashir A, Gray ML, Hartke J, Burstein D. Nondestructive imaging of human cartilage glycosaminoglycan concentration by MRI. Magn Reson Med 1999;41:857–65.
21. Kawamoto T. Use of a new adhesive film for the preparation of multi-purpose fresh-frozen sections from hard tissues, whole-animals, insects and plants. Arch Histol Cytol 2003;66:123–43.
22. Wakitani S, Goto T, Pineda SJ, Young RG, Mansour JM, Caplan AI, *et al*. Mesenchymal cell-based repair of large, full-thickness defects of articular cartilage. J Bone Joint Surg Am 1994;76:579–92.
23. Frazier SB, Roodhouse KA, Hourcade DE, Zhang L. The quantification of glycosaminoglycans: a comparison of HPLC, Carbazole, and Alcian blue methods. Open Glycosci 2008 Jan 1;1:31–9.
24. Kode JA, Mukherjee S, Joglekar MV, Hardikar AA. Mesenchymal stem cells: immunobiology and role in immunomodulation and tissue regeneration. Cytotherapy 2009;11:377–91.
25. Green WT. Articular cartilage repair. Behavior of rabbit chondrocytes during tissue culture and subsequent allografting. Clin Orthop Relat Res 1977:237–50.
26. Jamali AA, Emmerson BC, Chung C, Convery FR, Bugbee WD. Fresh osteochondral allografts: results in the patellofemoral joint. Clin Orthop Relat Res 2005:176–85.
27. Emmerson BC, Görtz S, Jamali AA, Chung C, Amiel D, Bugbee WD. Fresh osteochondral allografting in the treatment of osteochondritis dissecans of the femoral condyle. Am J Sports Med 2007;35:907–14.
28. Tanaka T, Komaki H, Chazono M, Fujii K. Use of a biphasic graft constructed with chondrocytes overlying a beta-tricalcium phosphate block in the treatment of rabbit osteochondral defects. Tissue Eng 2005;11:331–9.
29. Almqvist KF, Wang L, Wang J, Baeten D, Cornelissen M, Verdonk R, *et al*. Culture of chondrocytes in alginate surrounded by fibrin gel: characteristics of the cells over a period of eight weeks. Ann Rheum Dis 2001;60:781–90.
30. Gikas PD, Morris T, Carrington R, Skinner J, Bentley G, Briggs T. A correlation between the timing of biopsy after autologous chondrocyte implantation and the histological appearance. J Bone Joint Surg Br 2009;91:1172–7.
31. Bieri O, Scheffler K, Welsch GH, Trattnig S, Mamisch TC, Ganter C. Quantitative mapping of T2 using partial spoiling. Magn Reson Med 2011;66:410–8.
32. Revell CM, Athanasiou KA. Success rates and immunologic responses of autogenic, allogenic, and xenogenic treatments to repair articular cartilage defects. Tissue Eng Part B Rev 2009;15:1–15.
33. Burstein D, Velyvis J, Scott KT, Stock KW, Kim YJ, Jaramillo D, *et al*. Protocol issues for delayed Gd(DTPA)(2-)-enhanced MRI (dGEMRIC) for clinical evaluation of articular cartilage. Magn Reson Med 2001;45:36–41.
34. Williams A, Gillis A, McKenzie C, Po B, Sharma L, Micheli L, *et al*. Glycosaminoglycan distribution in cartilage as

determined by delayed gadolinium-enhanced MRI of cartilage (dGEMRIC): potential clinical applications. AJR Am J Roentgenol 2004;182:167–72.
35. Trattnig S, Marlovits S, Gebetsroither S, Szomolanyi P, Welsch GH, Salomonowitz E, *et al*. Three-dimensional delayed gadolinium-enhanced MRI of cartilage (dGEMRIC) for in vivo evaluation of reparative cartilage after matrix-associated autologous chondrocyte transplantation at 3.0T: preliminary results. J Magn Reson Imaging 2007;26:974–82.
36. Watanabe A, Wada Y, Obata T, Ueda T, Tamura M, Ikehira H, *et al*. Delayed gadolinium-enhanced MR to determine glycosaminoglycan concentration in reparative cartilage after autologous chondrocyte implantation: preliminary results. Radiology 2006;239:201–8.
37. Tiderius CJ, Olsson LE, Leander P, Ekberg O, Dahlberg L. Delayed gadolinium-enhanced MRI of cartilage (dGEMRIC) in early knee osteoarthritis. Magn Reson Med 2003;49:488–92.
38. Borthakur A, Mellon E, Niyogi S, Witschey W, Kneeland JB, Reddy R. Sodium and T1rho MRI for molecular and diagnostic imaging of articular cartilage. NMR Biomed 2006;19:781–821.
39. Duvvuri U, Reddy R, Patel SD, Kaufman JH, Kneeland JB, Leigh JS. T1rho-relaxation in articular cartilage: effects of enzymatic degradation. Magn Reson Med 1997;38:863–7.
40. Gold GE, Burstein D, Dardzinski B, Lang P, Boada F, Mosher T. MRI of articular cartilage in OA: novel pulse sequences and compositional/functional markers. Osteoarthritis Cartilage 2006;14(Suppl A):A76–86.
41. Insko EK, Kaufman JH, Leigh JS, Reddy R. Sodium NMR evaluation of articular cartilage degradation. Magn Reson Med 1999;41:30–4.
42. Wolff SD, Balaban RS. Magnetization transfer contrast (MTC) and tissue water proton relaxation in vivo. Magn Reson Med 1989;10:135–44.
43. Du J, Takahashi AM, Chung CB. Ultrashort TE spectroscopic imaging (UTESI): application to the imaging of short T2 relaxation tissues in the musculoskeletal system. J Magn Reson Imaging 2009;29:412–21.
44. Zhang K, Lu W, Marziliano P. Automatic knee cartilage segmentation from multi-contrast MR images using support vector machine classification with spatial dependencies. Magn Reson Imaging 2013;31:1731–43.